Glass transition as a topological phase transition

M. G. Vasin

Vereshchagin Institute of High Pressure Physics, Russian Academy of Sciences, 108840 Moscow, Russia

(Received 20 April 2022; revised 8 August 2022; accepted 21 September 2022; published 14 October 2022)

The glass transition is described as a phase transition in the system of topologically protected excitations in matter structure. The critical behavior of the system is considered in both static and dynamic cases. It is shown that the proposed model reproduces most of the characteristic thermodynamic and kinetic properties of glass transition: the Vogel-Fulcher-Tammann law, the behavior of susceptibility and nonlinear susceptibilities, and heat capacity behavior as well as the appearance of a boson peak in the frequency dependence of the dynamic structure factor near the glass transition temperature.

DOI: 10.1103/PhysRevE.106.044124

I. INTRODUCTION

Currently, glasses are commonly used in everyday life and technological applications. The glass state is also the subject of active studies in many areas of condensed matter physics. However, the microscopic mechanisms underlying this state of matter are still the subject of discussion.

There are many various approaches for solving the problem of description of glass transition by itself. A variety of ideas spread between two extreme points of view. On the one hand, assume that the glass transition is a purely kinetic effect, the result of dynamical locking of liquid disordering structure in the process of rapid quenching [1]. According to this approach, glass transition is a pronounced relaxation process which obeys kinetic laws. When approaching the liquid-to-glass transition, molecular rearrangements in glass-forming melts become so slow that the changes in structure do not have time to follow the decrease in temperature. The ratio of the structural relaxation time to the melt cooling rate plays a decisive role in this case [2], and the characteristic feature of the relaxation kinetics of glass-forming melts is the dynamic heterogeneity of the structure [3,4]. The significant progress of the kinetic theories is associated with the approaches based on the mode-coupling theory [5–7], in which dynamics is determined by static equilibrium averages. They start with Newton's equations of motion and end up with certain experimental predictions [8]. The mode-coupling theory predicts a critical temperature below which there is no presence of ergodic phase. The theory is believed to correctly explain the onset of viscous behavior upon cooling but is not so good at low temperatures [9]. The opposing hypothesis is that the critical slowing down is a consequence of an underlying or narrowly avoided phase transition [10,11], and the glass phase the result of a genuine thermodynamic phase transition to a disordered solid state [12,13]. These theoretical approaches also include one of the current most popular random first-order transition theories [14,15].

This article will provide arguments in favor of the second statement. Although at the liquid-glass transition the system has no any observable order parameter that changes during this transition, nevertheless one can claim it as one of the forms of thermodynamic phase transitions. In particular, in this paper, it will be shown that the transition to the glass phase can be described as a topological phase transition.

A topological phase transition is a phase transition between phases whose properties are not explained by standard arguments without involving the topological properties of systems. In our case, it will be considered the phase transition in a system of interacting topological defects (vortices), which leads to the appearance of a quasi-long order corresponding to a vortex system with an infinite correlation radius. This is a transition between two states of a system of topological defects: a state in which these defects are mobile, and a state in which they are frozen.

The basic idea behind this approach is not new. It is founded on the known fact that any liquid shows solid properties when probed on a sufficiently short timescale, its instantaneous local structure is similar to the order in solids, and its short-time elastic properties are characterized by the instantaneous elastic module. That is the basis of the wide class of elastic models which involve assumptions and reasoning also having a long history in the field of point defects in crystals [16]. The main point of one of the classes of these models was suggested beginning in a number of works in the late 1970s [17–20]. The physical properties of glasses are governed by an extended constituent, the odd line or disclination, which is the only structural element surviving the absence of generative homogeneity and the triviality of the space group [21]. The theoretical description of the glass phase as a frozen system of topologically stable defects was actively developed, for example, in [21–23]. The most attractive feature of this approach was universality, allowing one to describe glass transitions in various systems in terms of a common formalism. The idea that the transition to the glass state is a topological phase transition was suggested at around the same time [24].

In this paper, a further development of this approach is proposed. It is shown that a system of topological defects in a medium with a nonzero microscopic (or instantaneous)

shear modulus undergoes a phase transition, the theoretical description of which is reduced to a fairly simple statistical model. This phase transition is analogous in nature to the Berezinskii-Kosterlitz-Thouless transition in two-dimensional systems and is one of the forms of topological phase transitions. The presented analysis shows that most universal characteristic properties of glass transitions, including critical dynamics, can be described by this model.

The article is organized as follows: First, the theoretical model which considers the topologically protected perturbations as the main system's structural elements is formulated. These perturbations correspond to disclinations violating local symmetry concerning an axial rotation; Then the theoretical analysis of the critical behavior at the phase transition in the disclination subsystem is carried out. In the presented paper, we consider both the static and dynamic case. In the first case, the thermodynamic properties of the phase transition described by the model are calculated. In the second one, the frequency dependence of the dynamic structure factor of the system under consideration is determined.

II. MODEL

We consider a liquid in terms proposed by Frenkel [25]. This approach is based on the postulation of some similarity between crystals and liquids, and assumes the behavior of liquid particles at moderate temperatures is in a manner similar to ones in a crystal. However, while in crystals particles oscillate around their nodes, in liquids, after several periods, they change their positions.

This approaches validity by the fact that the liquid elastic properties clearly manifest on small space and timescales. In particular, at high frequencies in liquids, a finite value of the shear module and a solid-like oscillation spectrum are observed [26–33]. Since transverse phonons can exist in the liquid only at frequencies exceeding the value of the inverse relaxation time, which decreases with the temperature increasing, then the main criterion distinguishing a quasi-gas (soft) fluid from a solid-like one (Frenkel liquid) is one can count the zero value of the shear modulus in the entire possible frequency spectrum. On the phase diagram, the region of the crossover from one liquid type to another one is called a Frenkel line [34,35]. Accordingly, the system can be considered as a solid one if the shear modulus differs from zero on the entire scale of the measured frequencies.

Thus, at low temperatures according to the Frenkel approach, we consider a liquid as an elastic media containing both elastic and plastic deformations. The plastic deformation presence provides fluidity, and the elastic deformation defines the system's free energy.

The free energy density of a deformed elastic system is written as follows:

$$\mathcal{F} = \frac{\lambda}{2} u_{ll}^2 + \mu \hat{\mathbf{u}}^2, \tag{1}$$

where λ is the bulk modulus, μ is the instantaneous shear modulus, and $\hat{\mathbf{u}} = u_{ij} = du_j/dx_i = \nabla_i u_j$ is the distortion tensor ($\mathbf{u}$ is the strain vector). It should be noted that μ is the microscopic parameter, which corresponds to a macroscopic shear modulus in the case that the relaxation time of system structural surpasses by far the observation time. Since the shear modulus usually depends on the temperature and increases at the temperature decreasing, one can assume that in some temperature interval near glass transition this dependence constitutes a linear function: $\mu = \varepsilon(T_\mu - T)$, where T_μ is some effective temperature parameter. Then it is the temperature at which the shear elasticity appears in the liquid, and which corresponds to the Frenkel line [34,35] on the phase diagram. The condition of the zero value of the average (measured) static shear modulus of the system in the liquid state is satisfied at the accounting of the presence of movable plastic distortions in this system.

Thus, we consider liquid as elastic media, which is fluid because of the presence of many mobile plastic deformations corresponding to dislocations and disclinations. In the static consideration, the system is in mechanical equilibrium, and the $\mathbf{u}$ field is a free one. However, the elastic energy of this system is not zero since its nonordering structure is geometrically frustrated and contains stressful regions caused by the topologically protected distortions. The topologically protected rotation distortion corresponds to disclination (or vortex line), and for simplicity below we will consider only this distortion type. We also note since the disclination is caused by a violation of axial symmetry, then, according to topological laws, they are linear objects, and the field describing the interaction between them is Abelian.

Let the system contain a disclination in the point $\mathbf{r}_n$. It breaks the simple connectivity of the space and leads to appearing in the distortion tensor an irreducible part corresponding to the rotation at movement around this disclination:

$$\oint \hat{\mathbf{u}} d\mathbf{l} = \int \nabla \times \hat{\mathbf{u}}\, d^2\mathbf{r} = \mathbf{\Omega} \delta^{(2)}_{\mathbf{r}=\mathbf{r}_n}, \tag{2}$$

where the space integration is the integration over dimensionless variable $\mathbf{r}$: $V^{-1}\int dV = \int_{|\mathbf{r}|<1} d^3\mathbf{r}$, and $\mathbf{\Omega}$ is the Frank vector. It is well to bear in mind that it is a pseudovector.

If the system contains N disclinations, then the partition function can be represented in the form of the functional integral:

$$W = \int \mathcal{D}\hat{\mathbf{u}} \exp\left(-\beta \int d^3\mathbf{r}\, \mathcal{F}\right) \prod_{n=1}^{N} \delta\left(\mathbf{l} \cdot \nabla \times \hat{\mathbf{u}}_{\mathbf{r}_n} - \mathbf{\Omega} J_{\mathbf{r}_n}\right),$$

where $\beta = 1/k_b T$, $\delta(\ldots)$ is the functional delta function, $\mathbf{l}$ is the unit vector corresponding to the disclination $\mathbf{J}_\mathbf{r}$ direction, and $J_\mathbf{r} = \pm 1$ or 0. Using the integral representation of the delta function, one can represent the partition function of the system as follows:

$$W = \iint \mathcal{D}\hat{\mathbf{u}} \mathcal{D}\mathbf{A} \exp\left(-\beta \int d^3\mathbf{r}\, \mathcal{H}\right),$$

where $\mathbf{A}$ is an ancillary field, which forms the condition (2), and the effective Hamiltonian density of the system has the following form:

$$\mathcal{H} = \frac{1}{2}\mu \hat{\mathbf{u}}^2 + i\beta^{-1}\mathbf{A} \cdot \left(\mathbf{l} \cdot \nabla \times \hat{\mathbf{u}} - \mathbf{\Omega} \sum_{n=1}^{N} J \delta^{(2)}_{\mathbf{r}=\mathbf{r}_n}\right), \tag{3}$$

where N is the quantity of the disclination elements, and $\mathbf{r}_n$ ($n = 1, 2, \ldots, N$) are their coordinates. Note that the first term

of the free energy (1) is absent here, since the rotation tensor is nondiagonal.

After integration over the $\hat{\mathbf{u}}$ field, the system effective Hamiltonian density takes the following form:

$$\mathcal{H} = \frac{\beta^{-2}}{2\mu}(\nabla \times \mathbf{A})^2 - i\beta^{-1}\mathbf{\Omega A}\sum_{n=1}^{N} J\delta^{(2)}_{\mathbf{r}=\mathbf{r}_n}, \tag{4}$$

which corresponds to the system of vortices that interact by the $\mathbf{A}$ field. If one takes only two vortices and carries out integration over the $\mathbf{A}$ field, then one can be convinced that this interaction is the Coulomb one.

We consider the case of arbitrary vortices number. Therefore, we have to carry out averaging over the grand canonical ensemble of the vortices (see Appendix A). After this averaging, the system effective Hamiltonian density assumes the following form:

$$\mathcal{H} = \frac{\beta^{-2}}{2\mu}(\nabla \times \mathbf{A})^2 - g\beta^{-1}\cos(\mathbf{\Omega A}), \tag{5}$$

where g is the density of the vortex system. It is nothing else than the Hamiltonian density of the sine-Gordon theory [36,37].

Let us expand the cosine into the power series. The quantum field theory teaches us that in d-dimensional systems close to the critical point only the terms of the Taylor series expansion with powers of $\mathbf{A}$ less than $2d/(d-2) = 6$ are relevant [38]. It means that in the 3D case only the first two terms of this expansion are relevant, and the third one is marginal. Thus, the fluctuation corrections are relevant only for these first two terms, and the system effective Hamiltonian (5) density can be represented as follows:

$$\mathcal{H} = \frac{\beta^{-2}}{2\mu}(\nabla \times \mathbf{A})^2 + g\beta^{-1}(\mathbf{\Omega A})^2\left(\frac{1}{2} - \frac{(\mathbf{\Omega A})^2}{4!} + \frac{(\mathbf{\Omega A})^4}{6!}\right).$$

Let us separate the $\mathbf{A}$ field on fast, $\tilde{\mathbf{A}}$, and the slow, $\mathbf{A}$, parts: $\mathbf{A} \to \mathbf{A} + \tilde{\mathbf{A}}$, and average the model over $\tilde{\mathbf{A}}$. Since $\langle\tilde{\mathbf{A}}\rangle = 0$, the above expression is rewritten as follows:

$$\begin{aligned}\mathcal{H} = {} & \frac{\beta^{-2}}{2\mu}(\nabla \times \mathbf{A})^2 + g\beta^{-1}\frac{\Omega^2}{2}\mathbf{A}^2\left(1 - \frac{\Omega^2}{2}\langle\tilde{\mathbf{A}}\tilde{\mathbf{A}}\rangle_0\right) \\ & - g\beta^{-1}\frac{\Omega^4}{4!}\mathbf{A}^4\left(1 - \frac{\Omega^2}{2}\langle\tilde{\mathbf{A}}\tilde{\mathbf{A}}\rangle_0\right) + g\beta^{-1}\frac{\Omega^6}{6!}\mathbf{A}^6,\end{aligned} \tag{6}$$

where

$$\langle\tilde{\mathbf{A}}\tilde{\mathbf{A}}\rangle_0 = \lambda_D\int_0^{\lambda_D^{-3}}\frac{d^3\mathbf{q}}{(2\pi)^3}\frac{\mu\beta}{\mathbf{q}^2} = \int_0^1\frac{d^3\mathbf{p}}{(2\pi)^3}\frac{\mu\beta}{\mathbf{p}^2} = \frac{\mu\beta}{2\pi^2}, \tag{7}$$

λ_D is the Debye length, and $\mathbf{p}$ is the dimensionless momentum, $\mathbf{p} = \lambda_D\mathbf{q}$. It leads to the following effective Hamiltonian density presentation:

$$\begin{aligned}\mathcal{H} = {} & \frac{\beta^{-2}}{2\mu}(\nabla \times \mathbf{A})^2 + M^2\left(\frac{1}{2}(\Omega\mathbf{A})^2 - \frac{1}{4!}(\Omega\mathbf{A})^4\right) \\ & + g\beta^{-1}\frac{\Omega^6}{6!}\mathbf{A}^6,\end{aligned} \tag{8}$$

where $M^2 = g\Omega^4\varepsilon(T - T_0)/(2\pi)^2$ is the square of the effective $\mathbf{A}$ field "mass," and

$$T_0 = \frac{T_\mu}{1 + \frac{k_b}{\varepsilon}\left(\frac{2\pi}{\Omega}\right)^2} \tag{9}$$

is the phase transition temperature in the disclination subsystem. It is important that from the above derivation T_0 is proportional to the shear modulus of the glass state in T_0, $T_0 = \mu(T_0)(\Omega/2\pi)^2/k_b$, that is known experimental fact [39]. It is means that T_0 is the well-determined thermodynamic value of the condensed system, which directly relates with its elastic properties. From (8) one can see that T_0 is the tricritical point in the $\mathbf{A}$-field subsystem [40], since the factors of the quadratic and quartic powers of the $\mathbf{A}$ field simultaneously zeroing at $T = T_0$.

To understand what is the gist of this phase transition, one needs to revisit the (4) expression, from which one can see that the $\mathbf{A}$ field is the interaction field between the J particles. One can see this field is analogous to the vector potential of the electromagnetic field of a current, with the only difference that it is massive. As a result, the interaction between vortices is short range, and the vortex subsystem is a fluid of weakly coupled particles. The phase transition occurs at $T = T_0$, when the $\mathbf{A}$ field becomes massless, and the corresponding interaction becomes long range. The netlike phase of strong-coupled disclinations forms. One can see that this is a topological phase transition. By definition, a topological phase transition is a phase transition between phases whose properties are not explained by standard arguments without involving the topological properties of systems. In our case, this is a phase transition in a system of interacting topological defects (vortices), which leads to the appearance at a finite temperature of a quasi-long order corresponding to a vortex system with an infinite correlation radius. That is, it is a transition between two states of a system of topological defects: a state in which these defects are mobile, and a state in which they are frozen.

The $\mathbf{A}$ field corresponds to the gauge field of the vortex-vortex interaction in [20–24,36]. This field is arbitrary. Therefore, one can choose it in Coulomb gauge, $\nabla \cdot \mathbf{A} = 0$. Then the correlation function of the $\mathbf{A}$ field corresponding to the above Hamiltonian is

$$\langle\mathbf{AA}\rangle_{\mathbf{p}} = \frac{\beta}{\mu^{-1}\mathbf{p}^2 + \beta^2 M^2}.$$

It is not difficult to check that the static shear modulus $\mu_{st} \sim \mathbf{p}^2\langle\mathbf{AA}\rangle_{\mathbf{p}}|_{\mathbf{p}\to 0} = 0$ when $T > T_0$, and $\mu_{st} = \mu(T_0) \neq 0$ in $T = T_0$. Thus, from the definition of difference between liquid and glass states, it means that T_0 can be interpreted as the liquid-to-glass transition temperature.

One should recall that the above description of the system is correct only in the temperature region $T_\mu < T \geqslant T_0$, where the disclination system can be described in the framework of equilibrium statistical mechanics.

III. CRITICAL BEHAVIOR OF THE VORTEX SYSTEM NEAR T_0

In momentum space the pair correlation function of the vortices is

$$\langle \mathbf{JJ}\rangle_{\mathbf{p}} \propto \exp\left(\frac{\Omega^2\beta}{\mu^{-1}\mathbf{p}^2+\beta^2M^2}\right)$$

(see Appendix B). This function allows estimates of the correlation length of the vortices with opposite charges. We suppose that the vortex subsystem above T_0 presents a vortex liquid. Therefore, for the estimation we use the simplest form of a correlation function, which in liquids is exponentially decreasing with distance $|\langle \mathbf{JJ}\rangle|_{\mathbf{r}} \propto \exp(-|\mathbf{r}|/L_c)$ [40], where L_c is the correlation length. Thus,

$$L_c \propto |\langle \mathbf{JJ}\rangle|^{1/3}_{p=0} = \exp\left[\frac{k_b}{3g\varepsilon}\left(\frac{2\pi}{\Omega}\right)^2\frac{T}{T-T_0}\right]$$

(see Appendix C).

At first glance, it may seem strange that the vortex correlation length increases according to the faster law than the **A**-field correlation length. However, it is not difficult to understand this, if we remember that the **A** field describes the interaction between vortices. Therefore, the correlation length of the **A** field is the radius of interaction between vortices, which is not the correlation length of the vortices but is associated with it by more complex nonlinear relations. An increase of this radius leads to an increase in the effective number of nearest neighbors of each vortex, which reduces the percolation threshold and dramatically increases the size of the percolation region, which is much greater than this radius. Thus, the vortex correlation length grows faster than the interaction radius.

Unfortunately, the vortex correlation length as well as $\langle \mathbf{JJ}\rangle$ and $\langle \mathbf{AA}\rangle$ correlation functions cannot be directly observed in an experiment. However, there are other quantities connected with them which can be directly measured. Foremost, from the critical dynamics, it follows that the vortex correlation length connected with the relaxation time of the system, $\tau \propto L_c^z$, where z is the dynamical exponent. Therefore,

$$\tau \propto \exp\left[\frac{zk_b}{3g\varepsilon}\left(\frac{2\pi}{\Omega}\right)^2\frac{T}{T-T_0}\right], \tag{10}$$

which is nothing other than the Vogel-Fulcher-Tammann (VFT) law for the temperature dependence of the relaxation time near the glass transition point, and T_0 corresponds to the Vogel-Fulcher temperature being determined in experiment. At first sight, this seems to be surprising, since the VFT law is characteristic of frustrated systems near the glass transition. However, this is quite natural since the vortex-vortex interaction, described by the **A** field, like the Coulomb one is long-range, and the systems with a long-range interaction are frustrated [41,42]. Thus, the description of the interaction in terms of the gauge field **A** allows using the methods of equilibrium statistical mechanics for the description of systems with long-range interaction.

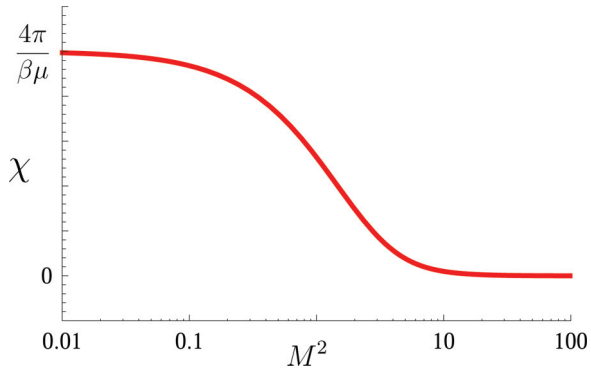

FIG. 1. Graphical illustration of the susceptibility change at the glass transition in the presented theoretical description (with a logarithmic M^2 axis).

A. Susceptibility

To derive the expression for linear and nonlinear susceptibilities of the system near T_0, let us follow the standard way and add to our system an external force; thus the Hamiltonian of the system is rewritten as follows:

$$\mathcal{H} = \frac{\mu}{2}\hat{\mathbf{u}}^2 + i\beta^{-1}\mathbf{A}\cdot\left(\mathbf{l}\cdot\nabla\times\hat{\mathbf{u}} - \mathbf{\Omega}\sum_{n=1}^{N} J\delta^{(2)}_{\mathbf{r}=\mathbf{r}_n}\right) + \hat{\sigma}\cdot\hat{\mathbf{u}}, \tag{11}$$

where $\hat{\sigma}$ is the externally induced stress tensor per unit volume, which after the calculation is supposed to be zero. The linear susceptibility can be derived by the differentiation $\chi = \partial_{\mathbf{f}}\langle \mathbf{u}\rangle$, where $\mathbf{f} = \nabla\cdot\hat{\sigma}$ is an external force. One can ascertain it is proportional to the $\langle \mathbf{uu}\rangle_{\mathbf{p}=0} = \mathbf{p}^{-2}\langle \hat{\mathbf{u}}\hat{\mathbf{u}}\rangle_{\mathbf{p}}|_{\mathbf{p}=0}$ correlation function. Since $\hat{\mathbf{u}}$ is the antisymmetric tensor corresponding to the local rotation of the media on some angle ω, $\omega_i = \varepsilon_{ijk}u_{jk}$, using the manipulations presented in Appendix D, one finds that

$$\begin{aligned}\langle \mathbf{uu}\rangle_{\mathbf{p}} &= \frac{1}{\mathbf{p}^2}\left[\left(\frac{1}{\beta\mu}\right)^2\mathbf{p}^2\langle \mathbf{AA}\rangle_{\mathbf{p}} + \frac{1}{\beta\mu}\right]\\ &= \frac{1}{\beta\mu}\left(\frac{\mu^{-1}}{\mu^{-1}\mathbf{p}^2+\beta^2M^2} + \frac{1}{\mathbf{p}^2}\right).\end{aligned}$$

As a result, one can write the expression for the dislocation contribution to susceptibility as follows:

$$\begin{aligned}\Delta\chi &= \int_0^1 d^3\mathbf{r}\langle \mathbf{uu}\rangle_{\mathbf{r}} = \frac{4\pi}{\beta\mu}\int_0^1 dr\, r[\exp(-r\sqrt{\mu}\beta M)+1]\\ &= \frac{4\pi}{\beta\mu}\left(\frac{1}{2} + \frac{1-(1+\sqrt{\mu}\beta M)\exp(-\sqrt{\mu}\beta M)}{\mu\beta^2M^2}\right).\end{aligned}$$

One can see that near T_0, when $M\to 0$, this value does not divergent (see Fig. 1). This is in agreement with experimental observations and highlights that the glass transition is not a second-order phase transition.

B. Nonlinear susceptibilities

In the glasses, the particularly interesting ones are third- and fifth-order susceptibilities. It is supposed that their divergence at the glass transition temperature is evidence that the

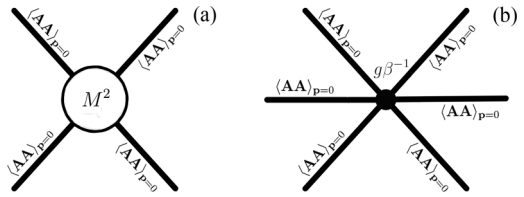

FIG. 2. (a) The four bold lines in the graph correspond to the correlation functions $\langle \mathbf{AA} \rangle_{\mathbf{p}}$, which cross in the vertex, M^2, corresponding to the $\mathbf{A}^4$ term of the effective Hamiltonian. (b) Six bold lines corresponding to the correlation functions graphs cross in the vertex, $g\beta^{-1}$, corresponding to the $\mathbf{A}^6$ term.

glass transition is a phase transition and points to the growth of thermodynamic amorphous order in glass formers.

The third-order nonlinear susceptibility χ_3 is proportional to the quadruple correlator of the $\mathbf{u}$ field: $\chi_3 = \partial_{\mathbf{f}}^3 \langle \mathbf{u} \rangle_{\mathbf{p}=0} \propto \langle \mathbf{u}^4 \rangle_{\mathbf{p}=0}$, which can be represented in the following form (see Appendix D):

$$\langle \mathbf{u}^4 \rangle_{\mathbf{p}=0} = \mathbf{p}^{-4} \langle \hat{\mathbf{u}} \rangle_{\mathbf{p}} |_{\mathbf{p}=0} = \left(\frac{1}{\beta\mu} \right)^4 \langle \mathbf{A}^4 \rangle_{\mathbf{p}=0} + 3 \langle \mathbf{uu} \rangle_{\mathbf{p}=0}^2.$$

Using the above susceptibility calculation, one can see that the second term in this expression gives finite contributions in contrast to the first term, which diverges at $T \to T_0{}^+$. Indeed, the irreducible part of the quadruple correlator $\langle \mathbf{A}^4 \rangle$, which graphically is represented in Fig. 2, is written as follows:

$$\langle \mathbf{A}^4 \rangle_{\mathbf{p}=0} \propto \left(\frac{1}{M^2} \right)^4 M^2.$$

As a result, $\chi_3 \propto \langle \mathbf{A}^4 \rangle_{\mathbf{p}=0} \propto (T - T_0)^{-3}$. Similarly, the fifth-order susceptibility is presented as follows:

$$\chi_5 \propto \langle \mathbf{A}^6 \rangle_{\mathbf{p}=0} \propto \left(\frac{1}{M^2} \right)^6 \propto \frac{1}{(T - T_0)^6}.$$

This result is consistent with $\chi_5 \propto \chi_3^2$ and supports a picture of amorphous compact domains mostly independent of differences at the molecular level [12,13].

C. Heat capacity

As noted above, the critical point in the $\mathbf{A}$-field subsystem is the tricritical point. The form of the corresponding thermodynamic potential (see Fig. 3) evidences the differences in the critical behavior of the system above and below the

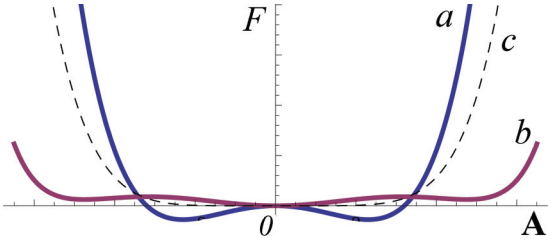

FIG. 3. Schematic drawing of the thermodynamic potential of the system with Hamiltonian (8) at the temperatures near T_0 (a) at the temperatures $T < T_0$, (b) at the temperatures $T > T_0$, and (c) at $T = T_0$.

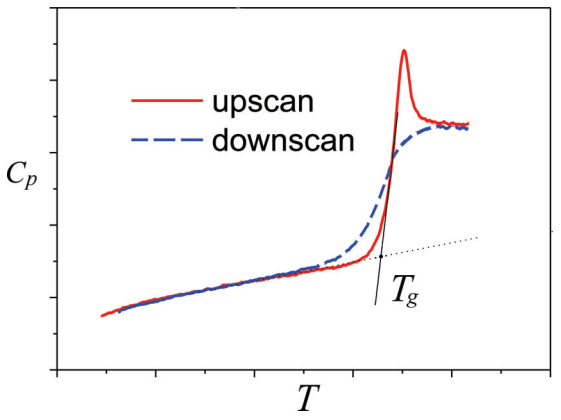

FIG. 4. Schematic drawing of the specific heat near the glass transition by cooling from the liquid phase (blue line) and subsequently reheating (red line) [16]. On cooling near the glass transition temperature T_g the specific heat fast decreases. On reheating, the specific heat follows a different path. It has a sharp increase, resembling the specific heat peak happening at the second-order phase transition.

glass transition temperature T_0. These differences are well known [40]. From Fig. 3 one can see that at the approach to T_0 from above, the system's criticality corresponds to a weak first-order phase transition, while at the approach to T_0 from below, the transition demonstrates the characteristic properties of the second-order phase transition. Thus, one can expect that the temperature dependence of the heat capacity of the considered system will demonstrate a sharp peak at $T \to T_0{}^-$, analogous to one at a second-order phase transition, but at $T \to T_0{}^+$ it will be a finite jump [40]. The behavior of this subsystem indeed qualitatively describes experimental observation of the heat capacity near a glass transition.

Knowing the partition function W one can estimate the vortex subsystem contribution to the heat capacity. At the approach to T_0 from below, it is written as follows (see Appendix E):

$$\Delta C_p^- = \frac{1}{\beta} \frac{\partial^2 (T \ln W)}{\partial T^2} \propto \frac{1}{|T_0 - T|^{1/2}}.$$

One can see it diverges as well as when at a second-order phase transition.

At the approach to T_0 from above, the heat capacity behavior is different from the above. This case corresponds to the first-order phase transition in the $\mathbf{A}$-field subsystem, which can happen in the temperature interval from $T = T_{cr}$, when the energy of symmetrical and antisymmetrical states of the $\mathbf{A}$-field subsystem are equal (binodal), to $T = T_0$ when the energy barrier between these states vanishes (spinodal) (see Fig. 3). Pursuant to the theory of tricritical point [40] in this case the heat capacity has no singularity but at some temperature undergoes a jump down:

$$\Delta C_p^+ = C_p(\text{liquid}) - C_p(\text{glass}) \approx \frac{15}{2} \frac{g(\Omega^4 \varepsilon)^2}{k_b (2\pi)^4}. \tag{12}$$

The described above behavior agrees with experimental observations, which can be illustrated by the picture presented in Fig. 4. The pulling of the liquid-glass transition temperature to the lower temperature region, which is present in the

experiments and in the figure, can be explained by the well-known phenomenon of the dependence of the temperature of the liquid-glass transition on the quenching rate. One can show this is the result of the anomaly slowing of the relaxation processes near T_0 (see, for example, [43]). A detailed study of this problem is possible within dynamic theory, which will be considered below.

The derived expression for heat capacity (12) allows expressing the configuration entropy dependence in the temperature interval from T_{cr} to T_0 in the familiar way:

$$S_c = \int_{T_0}^{T} dT \frac{\Delta C_p(T)}{T} \approx \Delta C_p^+ \ln \frac{T}{T_0} \approx \Delta C_p^+ \frac{T - T_0}{T_0}.$$

From this one can see that T_0 is close to the Kauzmann temperature, T_K, at which an "ideal glass transition" would occur [44].

IV. DYNAMICS

In contrast to usual thermodynamic phase transitions, a glass transition has pronounced dynamical features displaying the slow non-Debye relaxation (α relaxation), the dependence of the glass transition temperature on quenching velocity, the boson peak presence in the dynamic structure factor of supercooled liquids, etc. Naturally, it forces us to think about the pure dynamical nature of the glass transition. However, the above topological approach allows much to unite the thermodynamic and dynamic concepts. To demonstrate this, we will consider the dynamic properties of a glass-forming system within the framework of the proposed approach.

On one hand, this dynamics is in many ways similar to the critical dynamics characteristic of systems undergoing a second-order phase transition. Foremost, these transitions have in common a critical slowdown of dynamics near the transition temperature. Above, we have already made an estimate of the relaxation time of our system and shown that it indeed experiences a critical growth, satisfying the well-known VFT ratio.

On the other hand, the topological phase transition we are considering is a more complex phenomenon compared to the second-order phase transition. From (3) it can be seen that the system is described by the three fields. Each of these fields has its own characteristic timescale (as well as spatial scale). As a result, several relaxation modes can reveal themselves in our system at different timescales.

According to (3) in momentum-frequency space, the expression for the renormalized strain vector correlation function can be represented in the following form:

$$\begin{aligned}\langle \mathbf{uu} \rangle &= \langle \tilde{\mathbf{u}}\tilde{\mathbf{u}} \rangle + \boldsymbol{\Omega}^2 \langle \tilde{\mathbf{u}}\hat{\mathbf{u}} \rangle \mathbf{p} \langle \tilde{\mathbf{A}}\tilde{\mathbf{A}} \rangle \langle \mathbf{JJ} \rangle \langle \tilde{\mathbf{A}}\tilde{\mathbf{A}} \rangle \mathbf{p} \langle \hat{\mathbf{u}}\tilde{\mathbf{u}} \rangle \\ &= \langle \tilde{\mathbf{u}}\tilde{\mathbf{u}} \rangle + \boldsymbol{\Omega}^2 \mu^2 \beta^2 \langle \tilde{\mathbf{u}}\tilde{\mathbf{u}} \rangle \langle \mathbf{JJ} \rangle \langle \tilde{\mathbf{u}}\tilde{\mathbf{u}} \rangle,\end{aligned}$$

where $\tilde{\mathbf{u}}$ and $\tilde{\mathbf{A}}$ are fast (nonrenormalized) parts of the $\mathbf{u}$ and $\mathbf{A}$ fields, respectively. Limited to the first terms of the above expansion, and using the correlation function of the fast part of the $\mathbf{A}$ field, in the time space representation it is rewritten as follows:

$$\langle \mathbf{uu} \rangle_t \approx \langle \tilde{\mathbf{u}}\tilde{\mathbf{u}} \rangle_t + \frac{\boldsymbol{\Omega}^2 \mu^2 \beta^2}{\tau} \int_0^t \langle \tilde{\mathbf{u}}\tilde{\mathbf{u}} \rangle_{t'} \langle \mathbf{JJ} \rangle_{t-t'} dt'.$$

The qualitative view of this function is presented in Fig. 5.

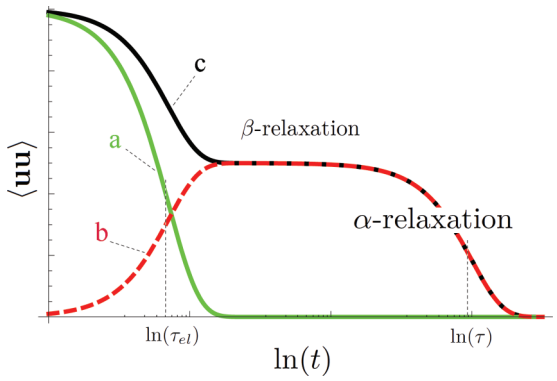

FIG. 5. Schematic drawing of $\langle \mathbf{uu} \rangle$ as a function of $\ln(t)$: (a) is the contribution $\langle \tilde{\mathbf{u}}\tilde{\mathbf{u}} \rangle$, which is the Debye relaxation; (b) is the contribution of the second term which is the cross-correlation of the $\langle \tilde{\mathbf{u}}\tilde{\mathbf{u}} \rangle_t$ and $\langle \mathbf{JJ} \rangle_t$ functions, which is given by the cooperative effects; (c) is the sum of the first and second terms.

From the figure one can see at the small timescales, $t < \tau_{el}$, where $\tau_{el} \sim \mu$ is the elastic relaxation time, the system demonstrates elastic properties which are characterized by the instant shear modulus. The system evolution on these timescales has the exponential form: $\langle \mathbf{uu} \rangle_t \sim \langle \tilde{\mathbf{u}}\tilde{\mathbf{u}} \rangle_t \propto \exp(-t/\tau_{el})$.

At the timescales comparable to the characteristic relaxation time of the vortex subsystem, $\tau_{el} \ll t \sim \tau$, the system kinetic properties are determined by the slow dynamics of vortices, $\langle \mathbf{JJ} \rangle_t \propto \exp(-t/\tau)$, corresponding to collective and strongly cooperative motion of many atoms or molecules, correlated on long-range scales. With time, the vortex subsystem evolves to an equilibrium state. This phenomenon proves itself as the final nonexponential decaying of the correlation function and is called the "α relaxation" [45]. Usually, the corresponding time dependence is approximated by the so-called Kohlrausch-Williams-Watts function, which has the following form: $\langle \mathbf{uu} \rangle_t \propto \exp[-(t/\tau)^b]$, where $b < 1$ (see Fig. 6).

At the medium timescales, $\tau_{el} < t \ll \tau$, at which the vortex subsystem have no time to relax, $\langle \mathbf{JJ} \rangle_t \sim \text{const} \neq 0$, the correlation function has a plateau which physical meaning is

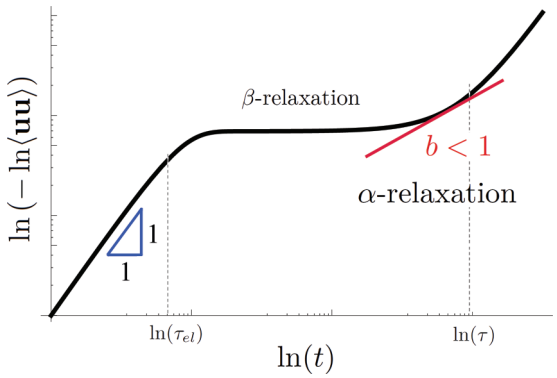

FIG. 6. Schematic drawing of $\ln(-\ln\langle \mathbf{uu} \rangle)$ as a function of $\ln(t)$, in which the straight line with b tilt corresponds to the $\exp[-(t/\tau)^b]$ function. One can see in the α-relaxation regime the relaxation is nonexponential, at $b < 1$ (the red tangent line). The regime with $b \approx 0$ at the medium timescales corresponds to the β relaxation.

given by the so-called "cage effect" [45]. In our interpretation, the size of this cage corresponds to the vortex correlation length. It means that for a short time interval the vortex system does not change, therefore the cooperative motion of atoms or molecules is blocked on macroscopic scales. Thus, the system is dynamically correlated and in the glasslike state existing during the short time $t < \tau$. On these timescales, the system demonstrates the characteristic for glasses' logarithmic relaxation (β relaxation).

A. Boson peak

One more dynamical property to examine is the so-called boson peak [46,47]. Usually, the boson peak is observed in the dynamic structure factor of supercooled liquids at temperatures below $T \approx 1.2\,T_g$ (T_g is the glass transition temperature). Its appearance is also related to the collective (dynamically correlated) motion of atoms and the formation of clusters with locally favored structures in the normal (quasi-gas) liquid medium. Recently, for example, the close link of the boson peak with the α relaxation was discussed using a system-bath coupling of the Zwanzig-Caldeira-Leggett type [48]. In our model, the vortex formation implies the presence of a locally ordered structure in which the vortex arises. Therefore, the size of the correlated clusters of this favored structure is defined by the vortex correlation length and **A**-field interaction radius. Thus, one can suppose that features of the low-frequency part of the absorption spectrum are related to the **A**-field mass renormalization.

For accurate analysis, we make use of the Keldysh-Schwinger technique. Before we turn to this technique, one should keep in mind that above during averaging over $\hat{\mathbf{u}}$ field, the system was supposed to be thermalized. Therefore, the subsequent consideration is correct in supposing that the **A** field is much slower than the $\hat{\mathbf{u}}$ field, which seems natural.

In the same way as above let us separate the $\hat{\mathbf{u}}$ and **A** fields on the fast, $\tilde{\mathbf{u}}$, $\tilde{\mathbf{A}}$, and the slow, $\hat{\mathbf{u}}$, **A**, parts: $\hat{\mathbf{u}} \to \hat{\mathbf{u}} + \tilde{\mathbf{u}}$, $\mathbf{A} \to \mathbf{A} + \tilde{\mathbf{A}}$. Let us suppose the fast parts of the fields are in thermal equilibrium, and average the model over $\tilde{\mathbf{u}}$ and $\tilde{\mathbf{A}}$ like in (8). Then, since $\langle\tilde{\mathbf{A}}\rangle = 0$, we can present the Hamiltonian of our system as follows:

$$\mathcal{H} = \frac{1}{2}\mu\hat{\mathbf{u}}^2 + i\mathbf{A}\cdot(\nabla\times\hat{\mathbf{u}}) + \frac{1}{2\mu}(\nabla\times\mathbf{A})^2 + M^2\left(\frac{1}{2}(\Omega\mathbf{A})^2 - \frac{1}{4!}(\Omega\mathbf{A})^4\right) + g\frac{\Omega^6}{6!}\mathbf{A}^6. \tag{13}$$

If we go over to the dynamic, in terms of the Keldysh-Schwinger technique [49–52] one can write the system's action functional in the following form:

$$\mathcal{S} = \frac{1}{2}\bar{\mathbf{u}}\hat{\Delta}_0^{-1}\bar{\mathbf{u}} + \frac{1}{2}\bar{\mathbf{A}}\hat{\mathbf{G}}_0^{-1}\bar{\mathbf{A}} + i\mathbf{A}\cdot[\nabla\times\hat{\mathbf{u}}'] + i\mathbf{A}'\cdot[\nabla\times\hat{\mathbf{u}}] - \gamma^{-1}M^2\frac{2\Omega^4}{4!}\mathbf{A}^3\mathbf{A}' + g\frac{2\Omega^6}{6!}\mathbf{A}^5\mathbf{A}', \tag{14}$$

where $\hat{\mathbf{u}}$ and $\hat{\mathbf{u}}'$ are the "quantum" and "classical" fields after the Keldysh rotation [50,51], $\bar{\mathbf{u}}$ is the vector $\bar{\mathbf{u}} = (\hat{\mathbf{u}},\ \hat{\mathbf{u}}')$, and $\hat{\Delta}_0$ is the prime Green function matrix which in momentum-frequency space the expression for the renormalized strain vector correlation function can be represented in the following

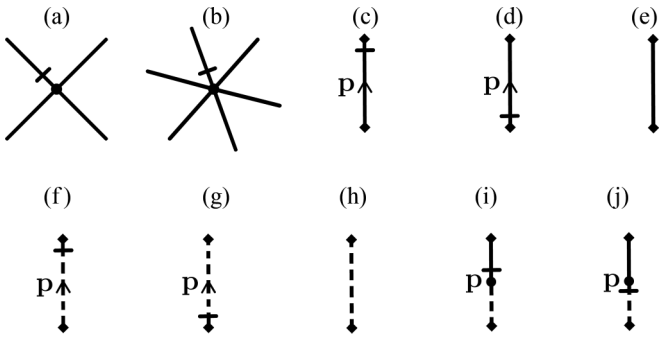

FIG. 7. The graphical presentation of the vertices $\mathbf{A}^3\mathbf{A}'$ (a) and $\mathbf{A}^5\mathbf{A}'$ (b), $[\mathbf{p}\times\hat{\mathbf{u}}']\mathbf{A}$ (j), $[\mathbf{p}\times\hat{\mathbf{u}}]\mathbf{A}'$ (i), and the prime Green functions G_0^A (c), G_0^R (d), G_0^K (e), Δ_0^A (f), Δ_0^R (g), and Δ_0^K (h).

form:

$$\hat{\Delta}_0 = \begin{bmatrix} \Delta^K_{0\,\mathbf{p},\,\omega} & \Delta^R_{0\,\mathbf{p},\,\omega} \\ \Delta^A_{0\,\mathbf{p},\,\omega} & 0 \end{bmatrix} = \begin{bmatrix} \frac{2\gamma k_b T}{\mu^2+\gamma^2\omega^2} & \frac{\gamma}{\mu-i\gamma\omega} \\ \frac{\gamma}{\mu+i\gamma\omega} & 0 \end{bmatrix}, \tag{15}$$

where γ is the kinetic coefficient, and Δ_0^R, Δ_0^A, Δ_0^K are respectively its retarded, advanced, and Keldysh components of $\hat{\Delta}_0$. Similarly, **A** and $\mathbf{A}'$ are the "quantum" and "classical" fields after Keldysh rotation, $\bar{\mathbf{A}}$ is the vector $(\mathbf{A},\ \mathbf{A}')$, and $\hat{\mathbf{G}}_0$ is the prime Green function matrix which in momentum-frequency space has the following form:

$$\hat{\mathbf{G}}_0 = \begin{bmatrix} G^K_{0\,\mathbf{p},\,\omega} & G^R_{0\,\mathbf{p},\,\omega} \\ G^A_{0\,\mathbf{p},\,\omega} & 0 \end{bmatrix} = \begin{bmatrix} \frac{2\gamma k_b T}{(\gamma^2\mu^{-1}\mathbf{p}^2+M^2)^2+\gamma^2\omega^2} & \frac{\gamma}{\gamma^2\mu^{-1}\mathbf{p}^2+M^2-i\gamma\omega} \\ \frac{\gamma}{\gamma^2\mu^{-1}\mathbf{p}^2+M^2+i\gamma\omega} & 0 \end{bmatrix}, \tag{16}$$

where G_0^R, G_0^A, G_0^K are respectively its retarded, advanced, and Keldysh components (see Fig. 7). Near the glass transition the **A**-field full correlation function matrix, $\hat{G}_{\mathbf{p},\,\omega}$, differs from the prime one by the addition of the self-energy term, $\Sigma_{\mathbf{p},\,\omega}$, to the **A**-field mass: $M^2 \to M^2_{R\,\mathbf{p},\,\omega} = M^2 - \gamma\,\Sigma_{\mathbf{p},\,\omega}$. Using the perturbation theory, one can find the dominant near T_0 contribution to self-energy is given by the logarithmically divergent term

$$\Sigma_{\mathbf{p},\,\omega} \approx \frac{M^4\Omega^4}{8\gamma^2}\iint\frac{d^3\mathbf{p}'d\omega'}{(2\pi)^4}\frac{d^3\mathbf{p}''d\omega''}{(2\pi)^4} \times G^K_{\mathbf{p}',\,\omega'}G^K_{\mathbf{p}'',\,\omega''}G^{A(R)}_{\mathbf{p}'+\mathbf{p}''+\mathbf{p},\,\omega'+\omega''+\omega},$$

which is graphically presented in Fig. 8. In the assumption of small M^2 in the $\mathbf{p} \to 0$ limit (see Appendix F)

$$\Sigma_{\mathbf{p}\approx 0,\,\omega} \approx M^4\frac{\mu^3}{\beta^2\gamma^7}\frac{\Omega^4}{8(2\pi)^2}\log\omega.$$

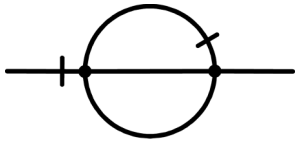

FIG. 8. This term gives a logarithmically divergent contribution to the M^2 renormalization.

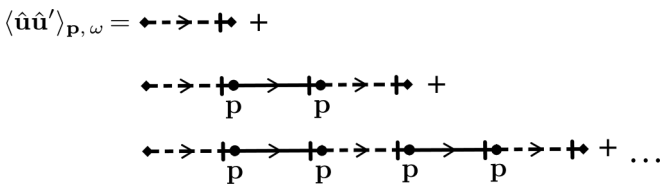

FIG. 9. Graphical presentation of the retarded component of the $\hat{\mathbf{u}}$-field Green function, which is a geometrical progression.

To determine the expression for the dynamic structure factor, $S(\omega)$, one should determine the Keldysh part of the time-dependent full correlation function matrix $\Delta^K_\omega = \langle \hat{\mathbf{u}}\hat{\mathbf{u}}\rangle_\omega \propto S(\omega)$. In momentum-frequency space, the retarded component of this matrix is written as follows (see Fig. 9):

$$\Delta^R_{\mathbf{p},\,\omega} = \Delta^{A^*}_{\mathbf{p},\,\omega} = \langle \hat{\mathbf{u}}\hat{\mathbf{u}}'\rangle_{\mathbf{p},\,\omega} = \frac{\gamma}{\mu - i\gamma\omega}\sum_{n=0}^{\infty}\left(\frac{\mathbf{p}^2\gamma G^R_{\mathbf{p},\,\omega}}{\mu - i\gamma\omega}\right)^n = \frac{\gamma}{\mu - \mathbf{p}^2 G^R_{\mathbf{p},\,\omega} - i\gamma\omega},$$

where G^R is the retarded component of the full $\mathbf{A}$-field Green functions matrix. Therefore, the Keldysh part of the time-dependent full correlation function matrix is

$$S(\omega) \propto \Delta^K_{\mathbf{p},\,\omega} = \frac{2\gamma\beta^{-1}}{\left|\mu - \mathbf{p}^2 G^R_{\mathbf{p},\,\omega} - i\gamma\omega\right|^2}. \tag{17}$$

Substituting the renumbered correlation function of the field $\mathbf{A}$, $G^R_{\mathbf{p},\,\omega}$, into this expression (see Appendix G) allows us to obtain the frequency dependence of the dynamic structure factor shown in Fig. 10. In the figure, one can see that the obtained function qualitatively exactly reproduces the character of the experimental frequency dependencies of the dynamic structure factor. The frequency peak corresponds to the intermolecular mode band. Its amplitude increases dramatically with increasing temperature, and the maximum shifts to low frequencies as expected for a collision-induced band. As can

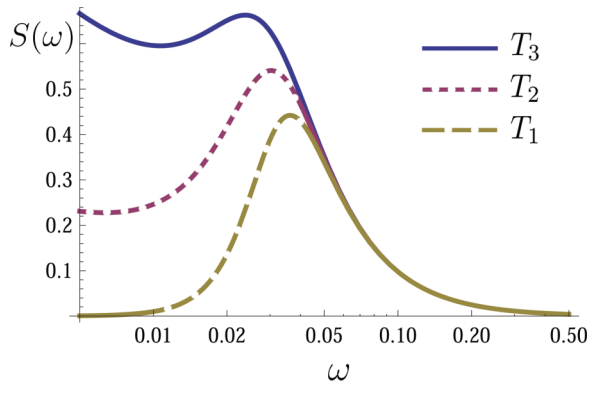

FIG. 10. The qualitative form of the frequency dependence of the dynamic structure factor, $S(\omega)$, derived with the (17) expression, with a logarithmic frequency axis ($T_1 \approx T_0 < T_2 < T_3$). With temperature growth, the peak maximum position shifts to low frequencies, and its height and width grow. At $T \to T_0$ the central peak vanishes. This picture qualitatively agrees well with experimental data (see, for example, [53]).

be expected, the vortex–vortex mutual scattering, being described by the $\Sigma_{\mathbf{p},\,\omega}$ term, corresponds to the collective or cooperative motion effect in which the intermolecular oscillation modes dominate. Exactly this contribution defines the Boson peak presence in the dynamic structure factor.

B. Motion equation of the Δ^K correlation function

In the conclusion of this section, we will discuss the connection of our theory with mode-coupling theory, which is the most developed theory for the evolution of glassy dynamics in liquids. For this, following [36,54] we write the Dyson equations for the correlation functions Δ^R and Δ^A:

$$\Delta^{R(A)} = \Delta_0^{R(A)} - \mathbf{p}^2\Delta_0^{R(A)} * G^{R(A)} * \Delta^{R(A)},$$

where the asterisk denotes the operation of convolution by t. Next, let us act on the Δ^R and Δ^A respectively by the operators $\hat{\Delta}_0^{-R} = \partial_t + \mu/\gamma$ and $\hat{\Delta}_0^{-A} = -\partial_t + \mu/\gamma$. Summing the results of these actions, one obtains the following expression (see Appendix H):

$$\hat{\Delta}_0^{-R}\Delta^R_{\mathbf{p},\,t} + \hat{\Delta}_0^{-A}\Delta^A_{\mathbf{p},\,t} = -\frac{2\mathbf{p}^2}{\tau}\int_0^t dt' G^R_{\mathbf{p},\,t-t'}\Delta^R_{\mathbf{p},\,t'}.$$

From this expression using the fluctuation-dissipation theorem, $\Delta^R - \Delta^A = \gamma\beta\partial_t\Delta^K$, we obtain the following equation (see Appendix H):

$$\gamma\partial_t^2\Delta^K_{\mathbf{p},t} + \mu\partial_t\Delta^K_{\mathbf{p},t} + \frac{\mathbf{p}^2}{\tau}\int_0^t dt' G^R_{\mathbf{p},t-t'}\partial_t\Delta^K_{\mathbf{p},t'} = 0,$$

which is the equation of motion for Δ^K_t in the Zwanzig-Mori representation of the mode-coupling theory [6]. One can see that the kernel function (memory function) of this equation is the $\mathbf{A}$-field correlation function, which just corresponds to the cooperative motion.

V. DISCUSSION

Various theoretical models and techniques are essentially different languages for describing some physical phenomenon. This description can have different sounds, but the content of the matter is the same. In the case of the glass transition, the common problem is the mathematical description of cooperative motion in disordered matter, accompanied by frustration and nonergodicity emergence. The theoretical approach presented in this paper considers this motion as the motion of topological vortices (disclinations) in a locally ordered elastic medium.

Comparing the topological approach presented here with mostly known ones, one should point out that it is closest ideologically to the theory of frustration limited domains [11,55–58] and is a development of the disclination model of glass [17–24] mentioned in introduction. Their general idea is the conception of geometrical frustration of glass structure, which arises at quenching and leads to the nonergodicity of the end state.

The presented picture well agrees with most modern theories, experimental data, and computer simulation results. For example, this topological picture naturally involves the dynamic heterogeneity widely discussed recently [59]. The point is that at the movement of the vortex, the most mobile atoms are close to its core. Thus, the moving vortices create around

themselves the areas of mobile atoms, which alternate with correlated slow areas. In our case, the spatial scale of this dynamic heterogeneity is comparable to the **A**-field correlation length.

Similar heterogeneity is also supposed in the popular random first-order transition theory, in which the supercooled liquid phase is thought to be composed of glassy clusters separated from each other. One supposes that these statistically similar incongruent global glassy metastable states appear at some temperature $T = T_A$ [14]. In our approach, the heterogeneity emergencies at the temperature $T = T_\mu$, when the vortices begin forming. The vortex subsystem is degenerate in energy because of numerous vortex configurations with equal energy, and the long-range Coulomb interaction between vortices leads to the system frustration [41,42]. Thus, one can see that T_μ and T_A are equivalent in nature.

By continuing to draw a parallel between our topological approach and the random first-order transition theory, attention must be paid to the similar results in the correlation length estimations. In the last one it is coherence length of the glass clusters, ξ [14], which can be obtained from computer simulation as a correlation of static shear deformations [60]. In our case, this correlation also can be determined as $\langle \mathbf{uu} \rangle$. From (17) one can see that in the static case, the correlation lengths of the **u** and **A** fields have equal asymptotic divergences at $T \to T_c$. In both cases $\xi \propto (T - T_0)^{-\nu}$. In the random first-order transition theory $\nu = 2/d \approx 0.67$, in our case with fluctuation corrections this value varies from $\nu \approx 0.67$ (3D XY model) to $\nu \approx 0.71$ (3D Heisenberg model [61]) depending on system symmetry. The computer modeling gives $\nu \approx 0.7$ [60]. One can see that these estimations are very close. At the same time, one should note that ξ is essentially different from the vortex correlation length estimated earlier, which grows much faster. The point is the last one is the percolation length in the system of arbitrary situated vortices where ξ is the length of local bonds between ones, and the percolation length grows faster than the bond length.

It is natural that both spatial and timescales have a dynamic heterogeneity effect on the system kinetics. Therefore, it is not surprising we found a direct connection between the **A**-field correlation function and memory function in the motion equation of the mode-coupling theory (MCT) [6]. One can hope that taking account of the system microscopic and topological properties in the framework of our approach will help to find the memory functions of MCT equations for a more precise description of the vitrification dynamics of real glass-forming systems.

VI. CONCLUSIONS

In conclusion, we summarize the main thesis of this work: the glass transition can be regarded as a topological phase transition. The key condition for the possibility of such a phase transition is the existence in liquid of nontrivial topologically protected structural excitations playing the role of quasiparticles, and the glass transition represents the condensation in the subsystem of quasiparticles.

The presented results of the theoretical analysis of the critical behavior of the proposed model allow us to assert that it gives an adequate description of most of the universal properties inherent in glass transitions in various systems. It describes the topological phase transition between disordered states of elastic condensed matter, which is characterized by the changing of the static shear modulus from $\mu_{st} = 0$, corresponding to high temperatures, to $\mu_{st} \neq 0$, corresponding to low ones. With this, the modulus scales with the glass transition temperature $\mu_{st} = \mu(T_0) \propto T_0$, which corresponds to the experimentally observed properties of glass transition.

It is shown that the distinctive feature of this phase transition, as the Berezinskii-Kosterlitz-Thouless transition in the two-dimensional XY model, is the absence of an order parameter. The long-range translational order does not occur during this transition, and the phase transition manifests itself in an infinite increase in the correlation radius and relaxation time as the system approaches the critical point. However, the divergence of the nonlinear susceptibility and a sharp peak in the temperature dependence of the heat capacity (in the case of an increase in temperature), derived in the framework of the model, as well as their experimentally observation, are confirmed by our conclusion that the glass transition is a special type of thermodynamic phase transition.

Since the interaction between quasi-particles (disclinations) is long-range, the properties of the systems consisting of them are largely determined by cooperative effects, which are especially strong on the kinetics of the system near the critical point. We can observe this both in the anomalous divergence of the relaxation time of the system according to VFT law and in the appearance of a boson peak in the low-frequency region of a dynamic structural factor. In turn, an abnormal relaxation slowdown leads to such experimentally observed effects as the dependence of the glass transition temperature on the cooling rate.

Thus, the proposed model can well describe both thermodynamic and kinetic properties of glass-forming systems. Considering the above, it can be argued that the model presented in the paper and its analysis prove the topological nature of glass transition.

ACKNOWLEDGMENT

I thank V. N. Ryzhov, V. M. Vinokur, and V. V. Brazhkin for stimulating discussions.

APPENDIX A

The system effective Hamiltonian has the following form:

$$\mathcal{H} = \frac{\beta^{-2}}{2\mu}(\nabla \times \mathbf{A})^2 - i\beta^{-1}\mathbf{\Omega A}\sum_{n=1}^{N} J\delta^{(2)}_{\mathbf{r}=\mathbf{r}_n}.$$

To take account of all possible vortices configurations, we carry out the averaging over a grand canonical ensemble of the "particles" endowed with the two possible dimensionless charges: $J_n = \pm 1$. Then the path integral is

$$W = \int \mathcal{D}A \left\{ \exp\left[-\beta \int d^3\mathbf{r}\, \frac{\beta^{-2}}{2\mu}(\nabla \times \mathbf{A})^2 \right] \times \sum_{N=1}^{\infty} \frac{(e^{-\beta\mathcal{E}_c})^N}{N!} \prod_{n=1}^{N} \int d^3\mathbf{r}_n \sum_{J_n=\pm 1} \exp\left[iJ_n \mathbf{\Omega A}(\mathbf{r}_n) \right] \right\}.$$

After summation, the system effective Hamiltonian density assumes the form

$$\mathcal{H} = \frac{\beta^{-2}}{2\mu}(\nabla \times \mathbf{A})^2 - g\beta^{-1}\cos(\mathbf{\Omega A}),$$

where $g = e^{-\beta\mathcal{E}_c}$ is the density of the vortex system. It is nothing other than the Hamiltonian density of the sine-Gordon theory.

APPENDIX B

Let us consider the correlation of the $\mathbf{J_p}$ vortices with some moment $\mathbf{p}$, when

$$\mathbf{J_p} = \int d^d\mathbf{r}\,\delta^{(2)}(\mathbf{r}-\mathbf{r}_n)\mathbf{J}_n e^{i\mathbf{p}\mathbf{r}} \approx J_n e^{i\mathbf{p}\mathbf{r}_n}.$$

In this case, the pair correlation function of the vortices is (see Fig. 11)

$$\begin{aligned}\langle \mathbf{J_p}\mathbf{J_{-p}}\rangle &= \langle \mathbf{J_p}\mathbf{J_{-p}}\exp[-i\mathbf{\Omega}(\mathbf{J_{-p}}\mathbf{A_p}+\mathbf{J_p}\mathbf{A_{-p}})]\rangle_A \\ &= \frac{\mathbf{J_p}\mathbf{J_{-p}}}{\int \mathcal{D}\mathbf{A}\exp[-\beta H]}\int \mathcal{D}\mathbf{A}\exp \\ &\quad\times[-\beta H + i\mathbf{\Omega}(\mathbf{J_{-p}}\mathbf{A_p}+\mathbf{J_p}\mathbf{A_{-p}})] \\ &= \mathbf{J_p}\mathbf{J_{-p}}\exp[-\mathbf{\Omega}^2\mathbf{J_p}\langle\mathbf{AA}\rangle_{\mathbf{p}}\mathbf{J_{-p}}] \\ &\propto \exp\left(-\frac{\mathbf{\Omega}^2 E\beta}{\mu^{-1}\mathbf{p}^2+M^2}\right).\end{aligned}$$

Another way to express the vortex correlator is the standard method by using an auxiliary field. In this case, the Hamiltonian (4) is rewritten as follows:

$$\mathcal{H} = \frac{\beta^{-2}}{2\mu}(\nabla\times\mathbf{A})^2 - i\beta^{-1}(\mathbf{\Omega A}+X)\sum_{n=1}^{N}\mathbf{J}\delta^{(2)}_{\mathbf{r}=\mathbf{r}_n},$$

and the correlator is expressed as

$$\langle\mathbf{JJ}\rangle_{\mathbf{r}-\mathbf{r}'} = -\frac{1}{W}\frac{\delta^2 W}{\delta X_{\mathbf{r}}\delta X_{\mathbf{r}'}}\bigg|_{X=0}.$$

After averaging over the grand canonical ensemble of vortices, the Hamiltonian is

$$\mathcal{H} = \frac{\beta^{-2}}{2\mu}(\nabla\times\mathbf{A})^2 - g\beta^{-1}\cos(\mathbf{\Omega A}+X).$$

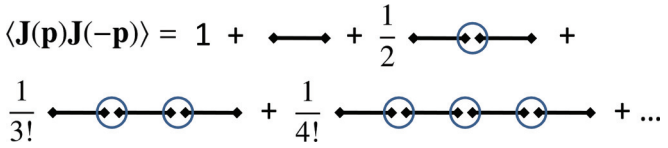

FIG. 11. Every dot corresponds to the *JA* vortex; every circle corresponds to the free vertices' correlation without interaction $\langle JJ\rangle_0 = \delta(\mathbf{r})$ $[\langle J(\mathbf{p})J(-\mathbf{p})\rangle_0 = 1]$.

Therefore,

$$\begin{aligned}\langle\mathbf{JJ}\rangle_{\mathbf{r}-\mathbf{r}'} &= -g^2\langle\sin(\mathbf{\Omega A_r})\sin(\mathbf{\Omega A_{r'}})\rangle \\ &= -\frac{g^2}{2}\langle\cos[\mathbf{\Omega}(\mathbf{A_r}-\mathbf{A_{r'}})]-\cos[\mathbf{\Omega}(\mathbf{A_r}+\mathbf{A_{r'}})]\rangle \\ &= \frac{g^2}{2}\exp\left[-\frac{\mathbf{\Omega}^2}{2}\langle(\mathbf{A_r}+\mathbf{A_{r'}})^2\rangle\right] \\ &\quad-\frac{g^2}{2}\exp\left[-\frac{\mathbf{\Omega}^2}{2}\langle(\mathbf{A_r}-\mathbf{A_{r'}})^2\rangle\right] \\ &= g^2\exp\left(-\frac{\mathbf{\Omega}^2}{2}\langle\mathbf{A}^2\rangle-\frac{\Omega^2}{2}\langle A^2\rangle\right) \\ &\quad\times\sinh(-\mathbf{\Omega}^2\langle\mathbf{AA}\rangle_{\mathbf{r}-\mathbf{r}'}) \\ &\approx -\frac{g^2}{2}\exp(-\mathbf{\Omega}^2\langle\mathbf{A}^2\rangle)\exp(\mathbf{\Omega}^2\langle\mathbf{AA}\rangle_{\mathbf{r}-\mathbf{r}'}).\end{aligned}$$

In momentum-frequency space, this correlator is written as follows:

$$\begin{aligned}\langle\mathbf{JJ}\rangle_{\mathbf{p}=0} &= \int d^3\mathbf{r}\langle\mathbf{JJ}\rangle_{\mathbf{r}} \propto \int d^3\mathbf{r}\exp(\mathbf{\Omega}^2\langle\mathbf{AA}\rangle_{\mathbf{r}}) \\ &= \int d^3\mathbf{r}\left(1+\mathbf{\Omega}^2\langle\mathbf{AA}\rangle_{\mathbf{r}}+\frac{\mathbf{\Omega}^4}{2}\langle\mathbf{AA}\rangle_{\mathbf{r}}^2+\cdots\right) \\ &= 1+\mathbf{\Omega}^2\langle\mathbf{AA}\rangle_{\mathbf{p}=0}+\frac{\mathbf{\Omega}^4}{2}\int\frac{d^3\mathbf{p}'}{(2\pi)^3}\langle\mathbf{AA}\rangle_{\mathbf{p}'}^2+\cdots \\ &\approx \exp(\mathbf{\Omega}^2\langle\mathbf{AA}\rangle_{\mathbf{p}=0}).\end{aligned}$$

APPENDIX C

We suppose that the vortex system presents a vortex liquid, therefore the spatial correlation of the vortices' density can be presented as the exponential function $|\langle\mathbf{JJ}\rangle|_{\mathbf{r}} \propto \exp(-|\mathbf{r}|/L_c)$ [40], where L_c is the correlation length. Thus,

$$\begin{aligned}\int d^3\mathbf{r}|\langle\mathbf{JJ}\rangle|_{\mathbf{r}} &\propto \int d^3\mathbf{r}\exp(-|\mathbf{r}|/L_c) \\ &= 4\pi\int drr^2\exp(-r/L_c) \\ &= 4\pi L_c^3\int dxx^2\exp(-x)\propto L_c^3.\end{aligned}$$

Then again,

$$\begin{aligned}\int d^3\mathbf{r}|\langle\mathbf{JJ}\rangle|_{\mathbf{r}} &= \int d^3\mathbf{r}\int_0^1\frac{d^3\mathbf{p}}{(2\pi)^3}|\langle\mathbf{JJ}\rangle|_{\mathbf{p}}e^{i\mathbf{p}\mathbf{r}} \\ &= \int_0^1 d^3\mathbf{p}|\langle\mathbf{JJ}\rangle|_{\mathbf{p}}\delta^{(3)}(\mathbf{p}) = |\langle\mathbf{JJ}\rangle|_{p=0}.\end{aligned}$$

Therefore, $L_c \propto |\langle\mathbf{JJ}\rangle|_{p=0}^{1/3}$.

APPENDIX D

After functional integration of the model with the Hamiltonian (11) over the $\hat{\mathbf{u}}$ field, the system effective Hamiltonian takes the following form:

$$\mathcal{H} = \frac{\beta^{-2}}{2\mu}(\nabla \times \mathbf{A} - i\beta\hat{\sigma})^2 - i\beta^{-1}\mathbf{\Omega A}\sum_{n=1}^{N} J\delta^{(2)}_{\mathbf{r}=\mathbf{r}_n}.$$

The sought-for correlation functions are found by the differentiation of the partition function over $\hat{\sigma}$ field.
The pair correlation function is derived by the double differentiation:

$$\langle \mathbf{uu}\rangle_{\mathbf{p}} = -\frac{1}{\mathbf{p}^2}\frac{\beta^{-2}}{W}\frac{\delta^2 W}{\delta\hat{\sigma}_{\mathbf{p}}\delta\hat{\sigma}_{-\mathbf{p}}}\bigg|_{\hat{\sigma}=0} = \frac{1}{\beta\mu}\left(\frac{1}{\beta\mu}\langle \mathbf{AA}\rangle_{\mathbf{p}} + \frac{1}{\mathbf{p}^2}\right),$$

and the quadratic correlation function is determined as

$$\begin{aligned}\langle \mathbf{u}^4\rangle_{\mathbf{p}} &= -\frac{1}{\mathbf{p}^4}\frac{\beta^{-4}}{W}\frac{\delta^4 W}{\delta\hat{\sigma}_{\mathbf{p}}\delta\hat{\sigma}_{\mathbf{p}}\delta\hat{\sigma}_{\mathbf{p}}\delta\hat{\sigma}_{\mathbf{p}}}\bigg|_{\hat{\sigma}=0}\\ &= \left(\frac{1}{\beta\mu}\right)^2\left[\left(\frac{1}{\beta\mu}\right)^2\langle \mathbf{A}^4\rangle_{\mathbf{p}} + 3\left(\frac{1}{\beta\mu}\right)^2\langle \mathbf{AA}\rangle^2_{\mathbf{p}}\right.\\ &\quad \left. + 6\frac{1}{\mathbf{p}^2}\frac{1}{\beta\mu}\langle \mathbf{AA}\rangle_{\mathbf{p}} + 3\frac{1}{\mathbf{p}^4}\right]\\ &= \left(\frac{1}{\beta\mu}\right)^4\langle \mathbf{A}^4\rangle_{\mathbf{p}=0} + 3\left[\frac{1}{\beta\mu}\left(\frac{1}{\beta\mu}\langle \mathbf{AA}\rangle_{\mathbf{p}} + \frac{1}{\mathbf{p}^2}\right)\right]^2\\ &= \left(\frac{1}{\beta\mu}\right)^4\langle \mathbf{A}^4\rangle_{\mathbf{p}} + 3\langle \mathbf{uu}\rangle^2_{\mathbf{p}}.\end{aligned}$$

APPENDIX E

According to the heat capacity definition, the contribution to this value of the vortex subsystem is

$$\begin{aligned}\Delta C_p &= \frac{1}{\beta}\frac{\partial^2(T\ln W)}{\partial T^2}\\ &= \frac{1}{\beta}\left[\frac{2}{W}\frac{\partial W}{\partial T} - T\left(\frac{1}{W}\frac{\partial W}{\partial T}\right)^2 + T\left(\frac{1}{W}\frac{\partial^2 W}{\partial T^2}\right)\right].\end{aligned}$$

By substituting the partition function W in this expression, one can estimate the heat capacity near T_0. At the approach to T_0 from below, the heat capacity is written as follows:

$$\begin{aligned}\Delta C_p &\approx \frac{k_b T^2}{W}\frac{\partial^2 W}{\partial T^2} = \frac{T}{2}\frac{\partial^2}{\partial T^2}\int\frac{d^3\mathbf{p}}{(2\pi)^3}\mu\langle \hat{\mathbf{u}}\hat{\mathbf{u}}\rangle_{\mathbf{p}}\\ &= \frac{T}{2}\frac{\partial^2}{\partial T^2}\int\frac{d^3\mathbf{p}}{(2\pi)^3}\left(\frac{\mathbf{p}^2(\beta\mu)^{-1}}{\mu^{-1}\mathbf{p}^2 + \beta^2 M^2} + \beta^{-1}\right)\\ &\approx \frac{T}{2\beta\mu}\frac{\partial^2}{\partial T^2}\int\frac{d^3\mathbf{p}}{(2\pi)^3}\frac{-M^2}{\mu^{-1}\mathbf{p}^2 + \beta^2 M^2} \propto \frac{1}{|T_0 - T|^{1/2}}.\end{aligned}$$

APPENDIX F

To calculate the following integral:

$$\begin{aligned}I^A(t) = \iint &\frac{d^3\mathbf{p}'d\omega'}{(2\pi)^4}\frac{d^3\mathbf{p}''d\omega''}{(2\pi)^4}\\ &\times G^K_{\mathbf{p}',\omega'}G^K_{\mathbf{p}'',\omega''}G^A_{\mathbf{p}'+\mathbf{p}'',\omega'+\omega''+\omega},\end{aligned}$$

it is convenient to consider it in the $(\mathbf{k},\ t)$ presentation:

$$\begin{aligned}I^A(t) = \beta^{-2}\iint &\frac{d^3\mathbf{k}}{(2\pi)^3}\frac{d^3\mathbf{k}'}{(2\pi)^3}\theta[t(\mu^{-1}(\mathbf{k}+\mathbf{k}')^2 + M^2)]\\ &\times\frac{\exp[-2\gamma\mu^{-1}(\mathbf{k}^2 - \mathbf{k}'\mathbf{k} + \mathbf{k}'^2)t - 3M^2 t\gamma^{-1}]}{(\gamma^2\mu^{-1}\mathbf{k}^2 + M^2)(\gamma^2\mu^{-1}\mathbf{k}'^2 + M^2)}.\end{aligned}$$

It can be integrated as follows:

$$\begin{aligned}I^A(t) &= \beta^{-2}\left(\frac{\mu}{\gamma^2}\right)^3\frac{(2\pi)^2}{(2\pi)^6}\int_0^1 dX\iint_{-\infty}^{\infty}dz\,dz'\theta[t(z^2 - 2z'zX + z'^2 + M^2)]\frac{z^2 z'^2\exp[-2\gamma^{-1}(z^2 - z'zX + z'^2)t - 3M^2 t\gamma^{-1}]}{(z+iM)(z-iM)(z'+iM)(z'-iM)}\\ &= \beta^{-2}\left(\frac{\mu}{\gamma^2}\right)^3\frac{(2\pi)^2}{(2\pi)^6}\int_0^1 dX\int_{-\infty}^{\infty}dz\,\theta[t(z^2 - 2iMzX)]\frac{-2\pi iM^2 z^2\exp[-2(z^2 - iMzX - M^2)t\gamma^{-1} - 3M^2 t\gamma^{-1}]}{2iM(z+iM)(z-iM)}\\ &= \beta^{-2}\left(\frac{\mu}{\gamma^2}\right)^3\frac{(2\pi)^2}{(2\pi)^6}\int_0^1 dX\pi^2 M^2\theta[t(2X-1)]\exp[-2(M^2X - M^2)t\gamma^{-1} - M^2 t\gamma^{-1}]\\ &= \beta^{-2}\left(\frac{\mu}{\gamma^2}\right)^3\frac{\pi^2 M^2}{(2\pi)^4}\int_0^1 dX\,\theta[t(2X-1)]\exp[-(2M^2X - M^2)t\gamma^{-1}]\\ &= \beta^{-2}\left(\frac{\mu}{\gamma^2}\right)^3\frac{1}{(2\pi)^2}\frac{\gamma}{8t}[\theta(-t)\exp(M^2 t\gamma^{-1}) - \theta(t)\exp(-M^2 t\gamma^{-1})].\end{aligned}$$

We take into account that $M^2 \ll 1$ and $\gamma > t$, thus

$$I^A(t) \approx -\theta(t)\beta^{-2}\left(\frac{\mu}{\gamma^2}\right)^3\frac{\gamma}{8(2\pi)^2}\frac{1}{t}.$$

After Fourier transformation

$$I^A(\omega) \approx \beta^{-2}\left(\frac{\mu}{\gamma^2}\right)^3\frac{\gamma}{8(2\pi)^2}(\log\omega + \mathcal{C}),$$

where $\mathcal{C}$ is Euler's constant, which can be neglected at small ω.

APPENDIX G

Near the glass transition, the **A**-field full correlation function matrix, $\hat{G}_{\mathbf{p},\omega}$, differs from the prime one by the addition of the self-energy term,

$$\Sigma_{\mathbf{p}\approx 0,\omega} \approx M^4 \frac{\mu^3}{\beta^2\gamma^7}\frac{\Omega^4}{8(2\pi)^2}\log\omega,$$

to the **A**-field mass, $M^2 \to M^2_{R\mathbf{p},\omega} = M^2 - \gamma\Sigma_{\mathbf{p},\omega}$:

$$\begin{aligned} G^R_{\mathbf{p},\omega} = G^{A*}_{\mathbf{p},\omega} &= \frac{\gamma}{\gamma^2\mu^{-1}\mathbf{p}^2 + M^2 - \gamma\Sigma_{\mathbf{p},\omega} - i\gamma\omega} \\ &= \frac{\gamma\left(\gamma^2\mu^{-1}\mathbf{p}^2 + M^2_{R\mathbf{p},\omega}\right)}{\left(\gamma^2\mu^{-1}\mathbf{p}^2 + M^2_{R\mathbf{p},\omega}\right)^2 + \gamma^2\omega^2} \\ &\quad + \frac{i\gamma^2\omega}{\left(\gamma^2\mu^{-1}\mathbf{p}^2 + M^2_{R\mathbf{p},\omega}\right)^2 + \gamma^2\omega^2}, \\ G^K_{\mathbf{p},\omega} &= \frac{2\gamma\beta^{-1}}{\left(\gamma^2\mu^{-1}\mathbf{p}^2 + M^2_{R\mathbf{p},\omega}\right)^2 + \gamma^2\omega^2}. \end{aligned}$$

As a result, the **u**-field full correlation functions have the following form:

$$\begin{aligned} \Delta^R_{\mathbf{p},\omega} = \Delta^{A*}_{\mathbf{p},\omega} &= \langle\hat{\mathbf{u}}\hat{\mathbf{u}}'\rangle_{\mathbf{p},\omega} = \frac{\gamma}{\mu - i\gamma\omega}\sum_{n=0}^{\infty}\left(\frac{\mathbf{p}^2\gamma G^R_{\mathbf{p},\omega}}{\mu - i\gamma\omega}\right)^n \\ &= \frac{\gamma}{\mu - \mathbf{p}^2\gamma G^R_{\mathbf{p},\omega} - i\gamma\omega}, \end{aligned}$$

$$\begin{aligned} \Delta^K_{\mathbf{p},\omega} = \frac{2k_bT}{\gamma\omega}\Im\left(\Delta^R_{\mathbf{p},\omega}\right) = 2\gamma k_bT\Bigg[\omega^2\gamma^2\left(1 + \mathbf{p}^2\frac{\beta\gamma}{2}G^K_{\mathbf{p},\omega}\right)^2 \\ + \left(\mu - \mathbf{p}^2\left(\gamma^2\mu^{-1}\mathbf{p}^2 + M^2_{R\mathbf{p},\omega}\right)\frac{\beta\gamma}{2}G^K_{\mathbf{p},\omega}\right)^2\Bigg]^{-1}. \end{aligned}$$

APPENDIX H

Let us act using the operator $\hat{\Delta}_0^{-R} = \partial_t + \mu/\gamma$ on $\Delta^R_{\mathbf{p},t}$:

$$\begin{aligned} \hat{\Delta}_0^{-R}\Delta^R_{\mathbf{p},t} &= \hat{\Delta}_0^{-R}\Delta^R_{0\mathbf{p},t} - \mathbf{p}^2\hat{\Delta}_0^{-R}\Delta^R_{0\mathbf{p},t} * G^R_{\mathbf{p},t} * \Delta^R_{\mathbf{p},t} \\ &= \delta_t - \mathbf{p}^2 G^R_{\mathbf{p},t} * \Delta^R_{\mathbf{p},t}, \end{aligned}$$

and the operator $\hat{\Delta}_0^{-A} = -\partial_t + \mu/\gamma$ on $\Delta^A_{\mathbf{p},t}$:

$$\begin{aligned} \hat{\Delta}_0^{-A}\Delta^A_{\mathbf{p},t} &= \hat{\Delta}_0^{-A}\Delta^A_{0\mathbf{p},t} - \mathbf{p}^2\hat{\Delta}_0^{-A}\Delta^A_{0\mathbf{p},t} * G^A_{\mathbf{p},t} * \Delta^A_{\mathbf{p},t} \\ &= \delta_t - \mathbf{p}^2 G^A_{\mathbf{p},t} * \Delta^A_{\mathbf{p},t}. \end{aligned}$$

Let us sum up the results of these actions, considering that $G^R_t = G^A_{-t} = \theta(t)e^{-t(M^2-\gamma\Sigma)}$, and $\Delta^R_t = \Delta^A_{-t} = \theta(t)e^{-t\tilde{\mu}}$, where $\tilde{\mu} \approx \mu + \mathbf{p}^2 G^R_{\mathbf{p},0}$ is the renormalized μ parameter. As a result, at $t > 0$ we obtain the following expression:

$$\begin{aligned} \hat{\Delta}_0^{-R}\Delta^R_{\mathbf{p},t} + \hat{\Delta}_0^{-A}\Delta^A_{\mathbf{p},t} &= \partial_t\left(\Delta^R_{\mathbf{p},t} - \Delta^A_{\mathbf{p},t}\right) + \frac{\mu}{\gamma}\left(\Delta^R_{\mathbf{p},t} + \Delta^A_{\mathbf{p},t}\right) \\ &= -\mathbf{p}^2\left(G^R_{\mathbf{p},t} * \Delta^R_{\mathbf{p},t} + G^A_{\mathbf{p},t} * \Delta^A_{\mathbf{p},t}\right) \\ &= -\frac{\mathbf{p}^2}{\tau}\int_0^t dt' G^R_{\mathbf{p},t-t'}\Delta^R_{\mathbf{p},t'} \\ &\quad - \frac{\mathbf{p}^2}{\tau}\int_{-t}^0 dt' G^A_{\mathbf{p},t-t'}\Delta^A_{\mathbf{p},t'} \\ &= -\frac{2\mathbf{p}^2}{\tau}\int_0^t dt' G^R_{\mathbf{p},t-t'}\Delta^R_{\mathbf{p},t'}. \end{aligned}$$

Using the fluctuation-dissipation theorem, $\Delta^R - \Delta^A = \gamma\beta\partial_t\Delta^K$, and bearing in mind that $G^A_t = \Delta^A_t = 0$ at $t > 0$, one obtains the following equation:

$$\gamma\partial_t^2\Delta^K_{\mathbf{p},t} + \mu\partial_t\Delta^K_{\mathbf{p},t} + \frac{\mathbf{p}^2}{\tau}\int_0^t dt' G^R_{\mathbf{p},t-t'}\partial_t\Delta^K_{\mathbf{p},t'} = 0,$$

which is the equation of motion in the Zwanzig-Mori representation of the mode-coupling theory.

[1] G. H. Fredrickson, Annu. Rev. Phys. Chem. **39**, 149 (1988).
[2] D. S. Sanditov and M. I. Ojovan, Phys.-Usp. **62**, 111 (2019).
[3] M. D. Ediger, Annu. Rev. Phys. Chem. **51**, 99 (2000).
[4] L. Berthier and G. Biroli, Rev. Mod. Phys. **83**, 587 (2011).
[5] W. Götze and L. Sjögren, Rep. Prog. Phys. **55**, 241 (1992).
[6] W. Götze, *Complex Dynamics of Glass-Forming Liquids: A Mode-Coupling Theory* (Oxford University Press, New York, 2009).
[7] A. P. Sokolov, Endeavour **21**, 109 (1997).
[8] S. P. Das, Rev. Mod. Phys. **76**, 785 (2004).
[9] C. Dreyfus and R. M. Pick, C. R. Acad. Sci., Ser IV: Phys., Astrophys. **2**, 217 (2001).
[10] J. P. Sethna, Europhys. Lett. **6**, 529 (1988).
[11] D. Kivelson, S. A. Kivelson, X. L. Zhao, Z. Nussinov, and G. Tarjus, Physica A **219**, 27 (1995); G. Tarjus, D. Kivelson, and P. Viot, J. Phys.: Condens. Matter **12**, 6497 (2000).
[12] S. Albert, Th. Bauer, M. Michl, G. Biroli, J.-P. Bouchaud, A. Loidl, P. Lunkenheimer, R. Tourbot, C. Wiertel-Gasquet, and F. Ladieu, Science **352**, 1308 (2016).
[13] G. Biroli, J.-P. Bouchaud, and F. Ladieu, J. Phys. Chem. B **125**, 7578 (2021).
[14] T. R. Kirkpatrick, D. Thirumalai, and P. G. Wolynes, Phys. Rev. A **40**, 1045 (1989).
[15] X. Xia and P. G. Wolynes, Proc. Natl. Acad. Sci. USA **97**, 2990 (2000).
[16] J. C. Dyre, Rev. Mod. Phys. **78**, 953 (2006).
[17] G. Toulouse, Comun. Phys. **2**, 115 (1977).
[18] J. Villain, J. Phys. C **11**, 745 (1978).
[19] E. Fradkin, B. A. Huberman, and S. H. Shenker, Phys. Rev. B **18**, 4789 (1978).
[20] N. Rivier Blackett, Philos. Mag. A **40**, 859 (1979).
[21] N. Rivier, Rev. Bras. Fis. **15**, 311 (1985).
[22] D. R. Nelson, Phys. Rev. B **28**, 5515 (1983).
[23] I. E. Dzyaloshinskii and G. E. Volovik, Ann. Phys. **125**, 67 (1980).
[24] I. E. Dzyaloshinskii and S. P. Obukhov, Sov. Phys. JETP **56**, 456 (1982).

[25] J. Frenkel, *Kinetic Theory of Liquids* (Oxford University Press, Oxford, 1947).

[26] M. Grimsditch, R. Bhadra, and L. M. Torell, Phys. Rev. Lett. **62**, 2616 (1989).

[27] T. Pezeril, C. Klieber, S. Andrieu, and K. A. Nelson, Phys. Rev. Lett. **102**, 107402 (2009).

[28] Y. H. Jeong, S. R. Nagel, S. Bhattacharya, Phys. Rev. A **34**, 602 (1986).

[29] S. Hosokawa, M. Inui, Y. Kajihara, K. Matsuda, T. Ichitsubo, W.-C. Pilgrim, H. Sinn, L. E. González, D. J. González, S. Tsutsui, and A. Q. R. Baron, Phys. Rev. Lett. **102**, 105502 (2009).

[30] V. M. Giordano and G. Monaco, Phys. Rev. B **84**, 052201 (2011).

[31] T. Scopigno, G. Ruocco, and F. Sette, Rev. Mod. Phys. **77**, 881 (2005).

[32] E. Pontecorvo, M. Krisch, A. Cunsolo, G. Monaco, A. Mermet, R. Verbeni, F. Sette, and G. Ruocco, Phys. Rev. E **71**, 011501 (2005).

[33] W.-C. Pilgrim, Chr. Morcel, J. Phys.: Condens. Matter **18**, R585 (2006).

[34] V. V. Brazhkin, A. G. Lyapin, V. N. Ryzhov, K. Trachenko, Y. D. Fomin, and E. N. Tsiok, Phys.-Usp. **55**, 1061 (2012).

[35] V. V. Brazhkin, Y. D. Fomin, A. G. Lyapin, V. N. Ryzhov, and K. Trachenko, Phys. Rev. E **85**, 031203 (2012).

[36] M. G. Vasin and V. M. Vinokur, Physica A **525**, 1161 (2019).

[37] P. Minnhagen, Rev. Mod. Phys. **59**, 1001 (1987).

[38] A. Zee, *Quantum Field Theory in a Nutshell* (Princeton University Press, Princeton, 2010).

[39] W. H. Wang, J. Appl. Phys. **99**, 093506 (2006).

[40] L. D. Landau, E. M. Lifshitz, *Course of Theoretical Physics. Statistical Physics* (Butterworth-Heinemann, Oxford, 1980), Vol. 5.

[41] D. Kivelson and G. Tarjus, J. Chem. Phys. **109**, 5481 (1998).

[42] P. A. Prudkovskii, A. N. Rubtsov, and M. I. Katsnelson, Europhys. Lett. **73**, 104 (2006).

[43] M. G. Vasin, J. Stat. Mech.: Theory Exp. (2011) P05009.

[44] F. H. Stillinger, J. Chem. Phys. **88**, 7818 (1988).

[45] W. Kob, in *Slow Relaxations and Nonequilibrium Dynamics in Condensed Matter*, edited by J. L. Barrat, M. Feigelman, J. Kurchan, and J. Dalibard Les Houches-École d'Été de Physique Theorique, vol. 77 (Springer, Berlin, 2002).

[46] G. Winterling, Phys. Rev. B **12**, 2432 (1975).

[47] U. Buchenau, M. Prager, N. Nücker, A. J. Dianoux, N. Ahmad, and W. A. Phillips, Phys. Rev. B **34**, 5665 (1986).

[48] B. Cui, R. Milkus, and A. Zaccone, Phys. Rev. E **95**, 022603 (2017).

[49] J. Schwinger, J. Math. Phys. **2**, 407 (1961).

[50] L. V. Keldysh, Sov. Phys. JETP **20**, 1307 (1965).

[51] A. Kamenev, *Field Theory of Non-equilibrium Systems* (Cambridge University Press, New York, 2011).

[52] K. A. Milton, *Schwinger's Quantum Action: From Dirac's Formulation through Feynman's Path Integrals, the Schwinger-Keldysh Method, Quantum Field Theory, to Source Theory Principle*, Springer Briefs in Physics (Springer, Cham, 2015).

[53] A. Farrell, M. G. Jiménez, N. Tukachev, D. A. Turton, B. A. Russell, S. Guinane, H. M. Senn, and K. Wynne, *Characterisation of the Boson Peak from the Glass Into the Liquid, ChemRxiv* (Cambridge Open Engage, Cambridge, 2021).

[54] D. R. Reichman and P. Charbonneau, J. Stat. Mech. (2005) P05013.

[55] L. Chayes, V. J. Emery, S. A. Kivelson, Z. Nussinov, and G. Tarjus, Physica A **225**, 129 (1996).

[56] D. Kivelson and G. Tarjus, Philos. Mag. B **77**, 245 (1998).

[57] F. Sausset, G. Tarjus, and P. Viot, Phys. Rev. Lett. **101**, 155701 (2008).

[58] S. Sachdev, Phys. Rev. B **33**, 6395 (1986).

[59] L. Berthier, G. Biroli, J. Bouchaud, L. Cipelletti, and W. Saarloos, *Dynamical Heterogeneities in Glasses, Colloids and Granular Media* (Oxford University Press, New York, 2011).

[60] M. Mosayebi, E. Del Gado, P. Ilg, and H. C. Őttinger, Phys. Rev. Lett. **104**, 205704 (2010).

[61] J. C. Le Guillou and J. Zinn-Justin, J. Phys. Lett. **46**, 137 (1985).